Journal of Environmental Radioactivity 151 (2016) 174–184

Contents lists available at ScienceDirect

Journal of Environmental Radioactivity

journal homepage: www.elsevier.com/locate/jenvrad

Origin of radon concentration of Csalóka Spring in the Sopron Mountains (West Hungary)

Ágnes Freiler [a, b, *], Ákos Horváth [a], Kálmán Török [b], Tamás Földes [c]

[a] Department of Atomic Physics, Eötvös Loránd University, Pázmány P. sétány 1/A, H-1117 Budapest, Hungary
[b] Geological and Geophysical Institute of Hungary, H-1145 Budapest, Stefánia út 14, Hungary
[c] Institute of Diagnostic Imaging and Radiation Oncology, University of Kaposvár, H-7400 Kaposvár, Hungary

ARTICLE INFO

Article history:
Received 23 April 2015
Received in revised form
30 September 2015
Accepted 4 October 2015
Available online xxx

Keywords::
Radon in spring water
Mylonitic gneiss
Emanation coefficient

ABSTRACT

We examined the Csalóka Spring, which has the highest radon concentration in the Sopron Mountains (West Hungary) (, yearly average of 227 ± 10 Bq L^{-1}). The main rock types here are gneiss and micaschist, formed from metamorphism of former granitic and clastic sedimentary rocks respectively. The aim of the study was to find a likely source of the high radon concentration in water.

During two periods (2007–2008 and 2012–2013) water samples were taken from the Csalóka Spring to measure its radon concentration (from 153 ± 9 Bq L^{-1} to 291 ± 15 Bq L^{-1}). Soil and rock samples were taken within a 10-m radius of the spring from debrish and from a deformed gneiss outcrop 500 m away from the spring. The radium activity concentration of the samples (between 24.3 ± 2.9 Bq kg^{-1} and 145 ± 6.0 Bq kg^{-1}) was measured by gamma-spectroscopy, and the specific radon exhalation was determined using radon-chamber measurements (between 1.32 ± 0.5 Bq kg^{-1} and 37.1 ± 2.2 Bq kg^{-1}). Based on these results a model calculation was used to determine the maximum potential radon concentration, which the soil or the rock may provide into the water. We showed that the maximum potential radon concentration of these mylonitic gneissic rocks (c_{pot} = 2020 Bq L^{-1}) is about eight times higher than the measured radon concentration in the water. However the maximum potential radon concentration for soils are significantly lower (41.3 Bq L^{-1}) Based on measurements of radon exhalation and porosity of rock and soil samples we concluded that the source material can be the gneiss rock around the spring rather than the soil there.

We determined the average radon concentration and the time dependence of the radon concentration over these years in the spring water. We obtained a strong negative correlation (−0.94 in period of 2007–2008 and −0.91 in 2012–2013) between precipitation and radon concentration.

1. Introduction

Radon is an inert gas, thus it can move trough porous system in soil or fragmented rock (Tanner, 1980; Soonawala and Telford, 1980; Csige, 2003; Somlai et al., 2011). Where the pores are saturated with water, radon is dissolved into the water and transported (Andrews and Wood, 1972). The concentration of radon in water varies within water types: surface waters, like lakes and rivers have the almost no radon concentration (Al-Masri and Blackburn, 1999; Somlai et al., 2011; Cosma et al., 2008), it is intermediate in general groundwater and the highest in uranium rich crystalline rocks (Akerblom and Lindgren, 1996; Przylibski et al., 2004).

Radon in natural springs may pose problems in radiological protection. The first is the direct ^{222}Rn ingestion during water consumption (Onishchenko et al., 2010). The European Commission recommendation is 100 Bq L^{-1} for ^{222}Rn in drinking water (European Commission, 2001). The second is the elevated ^{222}Rn concentration in the air of dwellings situated over the contaminated regions or areas with naturally high ^{226}Ra or ^{238}U content of the base (e.g. Gundersen, 1991; Onishchenko et al., 2010).

Several studies deal with the relationship of the radon concentration in water and the geological background. The high radon concentrations are usually measured in springs and wells discharging from granitic and metamorphic rocks. E.g. Weise et al. (2001) are dealing with the high radon concentration (1.7–2.2 kBq L^{-1}) in Einsenquelle water (Bad Bramac). This value is

* Corresponding author. Department of Atomic Physics, Eötvös Loránd University, Pázmány P. sétány 1/A, H-1117 Budapest, Hungary.
E-mail address: freiler.agnes@mfgi.hu (Á. Freiler).

http://dx.doi.org/10.1016/j.jenvrad.2015.10.004
0265-931X/

typical of the uranium-bearing granitic rock of this region. The uranium concent of the granitic rock here is 620 Bq kg^{-1}. Przylibski et al. (2004) showed that the groundwater discharging from granites and gneisses of the Polish part of the Sudety Mountains may have radon concentration exceeding 1000 Bq L^{-1}. Cosma et al. (2008) studied surface waters, well and spring waters in Transylvania and found that among the well waters and spring waters the highest radon concentrations (57–72 Bq L^{-1}) were measured where granitic formations were close (Cosma et al., 2008). 255–576 Bq L^{-1} radon concentration was measured in El Castano site where the springs discharging from granitic rocks (Horváth et al., 2010).

The Sopron Mountains is an interesting area in the northwestern corner of Hungary from point of view of radon since its geological background. The main rock types are gneiss and micaschists which formed from granitic and clastic sedimentary rocks. Some of the gneisses in the Sopron Mountains underwent plastic deformation which resulted in mylonite formation (Kisházi and Ivancsics, 1987, 1989). During this process fluids migrated through the mylonites and precipitated U and Th bearing minerals. This process may lead to increased radon exhalation ability of the rocks (Gundersen and Wanti, 1991).

Aros (2003) carried out a comprehensive survey on ^{222}Rn concentration of springs and the surrounding soils in the Sopron Mountains. She has taken water samples from 13 springs and the highest radon content was measured in Csalóka Spring (225 ± 8 Bq L^{-1}). The radon concentration range for the other springs was 2–165 Bq L^{-1}. She showed that soil near Csalóka Spring has higher ^{238}U content (116 Bq kg^{-1}) than the other soil samples from the Sopron Mountains (35–91 Bq kg^{-1}).

We chose this site for a detailed study since it has the highest radon concentration among the springs in previous studies and since the mylonitic deformation of gneiss country rock, which enhances migration of radon in its increased effective pore volume.

The goals of this study were i) to determine the average radon concentration over a year in the spring water, ii) the changes in radon concentration over a year in the spring water, iii) to determine what controls these changes. iv) to determine whether the soil or/and the rocks near to surface can be the source of this radon. To achieve these goals we measured the water radon content by liquid scintillation spectroscopy, the radium activity concentration of rock and soil samples by gamma-spectroscopy, and minimum specific radon exhalation using radon-chamber measurements. We also determined the bulk density and porosity of the rock and soil. Using these data model calculations were made to estimate the maximum potential radon concentration (c_{pot}), which can be provided by the soil or the rock to the water by their radon exhalation ability. The pH, temperature, specific electrical conductivity of the spring was measured from 2012 to 2013 every sampling days and water chemistry measurements were carried out in three cases.

2. Samples and measurement techniques

2.1. Sampling site and procedures

The Sopron area is the easternmost part of the Eastern Alps (Fig. 1). Several rock types including orthogneiss, micaschist, leucophyllite and amphibolite were described in the Sopron area (e.g. Lelkes-Felvári et al., 1984; Kisházi and Ivancsics, 1989; Draganits, 1998; Török, 1998, 1999, 2001).

Two different lithological units have been distinguished by Draganits (1998) in the Sopron area. The massive gneisses and garnet-bearing chlorite–muscovite–quartz schist in contact with them were termed as Sopron Series and the micaschist around Óbrennberg was called Óbrennberg–Kaltes Bründl series.

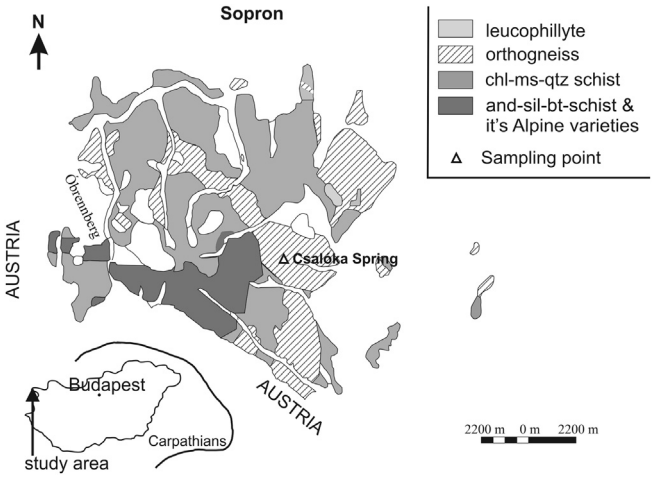

Fig. 1. Geologic map of the Sopron area showing the Csalóka Spring.

The metamorphic history of the Sopron area is quite complex, at least one pre-Alpine and an Alpine metamorphic stage was recorded. During the formation of the Sopron Mountains micaschist, the largest rock mass was the first to form from sedimentary rocks, then granitic rocks intruded into the micaschist and metamorphosed together during the Alpine orogeny. The Alpine metamorphism transformed the granitic rock into orthogneiss. The micaschist and orthogneiss underwent several secondary processes during the retrograde metamorphism, such as various degree of plastic deformation. Plastic deformation, also called mylonitisation at high pressures, is a process that takes place at temperatures over 250–300 °C, during which the rock structure rather then the mineral composition changes. Due to plastic deformation the rock fabric changes, it becomes striped/streaky, with preferred orientation, furthermore the originally large grains are crushed, broken down.

The Csalóka Spring is situated in the eastern part of the Sopron Series, at the top of the southern branch of the Iker-árok (ditch) and discharging from deformed mylonitic gneiss country rock (Fig. 1). Csalóka Spring is not a well defined spring since it discharges diffusely from the soil and flowing through the surface of the ditch (Fig. 2b). Water flow at point A is the main discharge of the Csalóka Spring (Fig. 2a & b). From point A the water flows down the surface of the ditch (through points F, G, H on Fig. 2a) and reach the other permanent water flow (creek) originating from point E, which is the starting point of the creek. During the soil sampling process 10–20 cm deep holes were made and the water accumulated in the hole. Three points; B, C, D (Fig. 2b) were selected around the spring as additional sampling points for water. During the year the presence of water in the B, C, D points was temporary.

To measure the radon concentration of the Csalóka Spring, altogether 31 water samples were collected from November 2007 to October 2008. Point A was sampled 13 times during a year. Point B was sampled 9 times; points C and D were sampled 2 times. The samples were taken by a 10 ml syringe to a 25 ml glass vial which has already contained 10 ml scintillation material, OptiFluor-O. The vials were sealed air tight using parafilm for this purpose.

Between 2012 and 2013 we have repeated the water sampling process from point A. Seven water samples were collected from November 2012 to July 2013. The water temperature and pH, were measured every sampling day by a Testo 206-pH1 portable instrument (accuracy: ±0.4 °C and 0.02). The specific electrical conductivity was measured, too (Table 3a). The flow velocity was roughly estimated once. A 1 L measuring cup was used and the time

Fig. 2. a. The photo of the sampling site. Letters indicates sampling points. b. Picture of the point A. c. DU deformed gneiss outcrop 500 m away from the spring and the place of rock sampling.

was measured while the water flowed to a known volume. Water chemistry measurements were made three times, after a spring, a summer and an autumn period (Table 3b).

To measure the radon exhalation of the soil and rocks around the Csalóka Spring 7 soil samples were collected with a spade from the surface to 40 cm depth from point A, B and D. No outcrops of the gneissic host rock were found within 20 m around the spring, thus we could collect these rock samples as debris. Eight rock samples originated form pont A, 1-1 from points J, K and I. Two soil samples are originating from point A, two from point B and 1-1 from points D, G, H, J.

There is an outcrop, (indicated by DU on Fig. 2a) just 500 m away from the Csalóka Spring where mylonitic gneiss as bedrock appears on the surface. We have collected 9 more rock samples from the outcrop to have representative samples of the surrounding rocks.

2.2. Sample preparation

2.2.1. Soil samples

After a 48 h drying at room temperature the soil samples were put into aluminium radon chambers. Radon chambers have the diameter of 7 cm and height of 9 cm with two taps.

2.2.2. Rock samples

The rock samples were cut to nearly cylindrical shapes with height of 4–5 cm and diameter of about 6–7 cm. Since the samples are deformed gneiss, their fabrics are orientated; three rock samples were cut in two different orientations: i) perpendicular to the orientation, ii) parallel to the orientation. We intended to check if the radon exhalation of the samples depends on the orientation.

Table 1
Specific radium activity, minimum specific radon exhalation and radon emanation coefficients of the soil and rock samples averaged for two independent measurements, and the porosities of rock samples. The first letters indicate S = soil and R = rocks samples, w indicates exhalation into water. ε = Radon emanation coefficient. Location of the samples beginning with DU is indicated on Fig. 2c.

Name of sample	Specific radium activity (Bq kg^{-1})	σ_{Ra} (Bq kg^{-1})	Minimum specific radon exhalation (M_{min}) (Bq kg^{-1})	σ_M (Bq kg^{-1})	ε (%)	σ_ε (%)	Porosity (%)
SA1	60.8	3.9	9.5	1.2	15.7	2.3	
SA1w			9.1	1.5			
SA2	65.8	5.1	6.3	1.0	9.6	1.7	
SB1	118	4.6	37.1	2.2	31.6	2.2	
SB2	145	6.0	13.2	1.3	9.1	1.0	
SD1	90.5	5.7	4.6	0.5	5.0	0.6	
SG1	75.5	5.0	14.7	2.5	19.5	3.6	
SH1	104	6.1	12.1	1.6	11.5	1.7	
SJ	46.8	2.4	5.0	0.6	10.7	1.4	
RA1V1	60.3	4.9	9.5	1.5	15.7	2.2	1.10
RA1V2	69.7	3.9	9.3	2.4	13.4	2.2	0.98
RA2V1	34.0	2.6	4.0	0.4	11.9	1.3	1.27
RA2V2	35.2	2.8	7.5	0.6	21.3	2.1	
RA3V1	77.9	3.7	8.8	0.7	11.3	0.9	1.52
RA3V2	81.7	5.0	10.4	1.4	12.8	1.7	1.80
RA4	56.5	3.9	5.1	0.7	9.8	1.5	
RA5	66.6	3.8	3.7	0.8	5.6	1.2	0.84
RA6	56.6	3.2	11.0	1.0	19.3	1.8	
RA7	69.9	3.1	15.7	0.9	22.4	1.6	
RA8	89.9	3.3	9.3	0.6	10.3	0.7	
RJ1	72.2	4.1	10.5	1.0	14.6	1.4	1.06
RK1	61.1	3.6	10.9	0.9	11.1	1.1	0.96
RI1	72.0	3.2	11.8	0.9	16.5	1.2	1.35
D2U3T	81.4	3.3	12.0	0.6	14.8	1.0	
D7U1V1	70.3	3.4	11.3	1.1	16.1	1.7	
D7U2V1	99.7	3.9	16.2	1.3	16.2	1.5	
D7U4V1	96.4	4.4	8.3	1.1	8.66	1.1	
D7U4V2	95.4	4.3	13.1	1.3	13.7	1.5	
D7U5V1	77.1	3.6	9.9	0.9	13.0	1.4	
D7U5V2	72.8	3.8	9.7	1.1	13.4	1.7	
D7U6V1	85.0	3.4	12.6	0.9	14.8	1.2	
D7U6V2	80.4	3.5	15.1	1.1	18.8	1.6	
D7U7V1	73.7	3.4	10.9	0.8	14.8	1.3	
D7U8V1	24.3	2.9	4.2	0.9	17.7	4.5	
D7U8V2	28.4	2.8	4.4	0.5	15.5	2.4	
DU2V1	69.6	3.1	12.0	0.9	17.3	0.7	
DU2V2	76.4	3.5	12.9	0.9	16.9	0.7	

2.3. Measurement techniques

2.3.1. Radon concentration of the water samples

The ^{222}Rn concentration in the water of the Csalóka Spring was determined by liquid scintillation spectroscopy using a TRI-CARB 1000 TR detector. Each measurement in the laboratory was 15 min long, and 25–900 keVee light output region was set. The machine was calibrated using aqueous radium chloride solutions of known concentration. The radon concentration of the sampled water was corrected for the time elapsed until the measurement.

2.3.2. Water chemistry measurements

The measurements were carried out in the Eötvös Loránd University, Department of Physical and Applied Geology. The Ca^{2+} and Mg^{2+} concentration was measured by titration techniques, Mg^{2+} concentration was calculated from the total hardness of the water. The Na^+ and K^+ ion concentration was measured by a FLAMOM type flame photometer. The HCO_3^- ion concentration was determined by titration with HCl, and the Cl^- ion concentration with $AgNO_3$. The SO_4^{2-}, NO_3^- and SiO_3^{2-} concentration was measured by a Spektromom 195D photometer (Eaton et al., 2005).

2.3.3. Radon exhalation

The specific radon exhalation (the exhaled radon atoms by a unit mass of the sample per second, M) of the soil and rock samples into air were estimated by radon chamber method. Each solid sample was placed into a radon chamber and then it was closed. After three weeks it reached the radioactive equilibrium between ^{222}Rn activity (A) and ^{222}Rn exhalation ($E = A$), and then we determined the radon concentration of the air above the sample in the chamber

Table 2
Measured and calculated radon concentration and minimum radon exhalation values.

Type of sample	Location	Number of samples	c_{meas} (Bq L^{-1})	Average minimum specific radon exhalation (Bq/kg)	Porosity (%)	Density (g cm^{-3})	$c_{pot,min}$ (Bq L^{-1})	$c_{pot,max}$ (Bq L^{-1})
Soil	A	2	227 ± 10	7.9 ± 2.3	44	1.46	26	**65**
	B	2	163 ± 9	25.2 ± 16.9	44	1.46	83	207
	D	1	21 ± 3	4.6 ± 0.6	44	1.46	15	37
Rock	A	8	227 ± 10	10.1 ± 1.0	1.21	2.42	**2020**	5050

Bold numbers belonging to point A, which is the main sampling point around Csalóka Spring. 65 Bq/L is the maximum value of the potential radon concentration originating from the soil. This proves that the soil cannot be the source of the radon. Besides, the minimum value from rock is one order of magnitude higher then the measured radon concentration.

Table 3a
Temperature, pH and specific electrical conductivity of the water samples.

Date of the measurement	T (°C)	σ_T (°C)	pH	σ_{pH}	EC at 20 °C (μS/cm)
2012.11.02.	9.95	0.07	5.72	0.10	154
2012.12.17.	8.30		5.68		142
2013.02.20.	7.45	0.21	5.49	0.18	142
2013.04.11.	6.55	0.35	5.52	0.30	138
2013.05.04.	8.60	0.42	5.29	0.18	138
2013.06.22.	10.7	0.49	5.68	0.01	205
2013.07.21.	11.0	0.40	5.19	0.13	149
2013.09.15.	11.9		4.98		142
2013.10.19.	11.0	0.07	5.33	0.20	143

($c_{air} = A/V_{net}$), where V_{net} is the free air volume in the chamber above the sample by RAD7 Electronic Radon Detector (Durridge Company Inc, 2000), which was connected to an aluminium radon accumulation chamber by a pipe system.

The exhalation of all samples was measured two times using different radon chambers to avoid accidental false measurements due to leakage. Back diffusion was minimized because the pore volume of the samples was at least 10 times smaller than the free volume of the chamber. This reduces the importance of the back diffusion to negligible, as it was showed by Samuelsson and Petterson (1984), Samuelsson and Erlandsson (1988), Samuelsson (1990). The instrument setting was "Sniff Mode" protocol, where the radon activity concentration is calculated from the ^{218}Po alpha peak at 6.1 MeV and the radon activity concentration is given in Bq m^{-3}. The measurement included four cycles, 15 min each, after a half an hour background measurement (c_b). The emanation depends on the humidity and as a trend saturetes at about 5%–10% (2.2.2. subchapter of review of Sakoda, 2011; Breitner, 2010) The humidity of the system was kept below 10% during the measurement, which means it was about or greater then 10% during the accumulation time. From the measured air radon concentration (c_m), which is actually a diluted air by the background radon concentration (c_b) the c_{air} can be calculated (Eq. (1)).

$$c_{air} = c_m\left(1 + \frac{V_{det}}{V_{net}}\right) - c_b\frac{V_{det}}{V_{net}} \quad (1)$$

where, V_{det} is the volume of the pipe system plus the inner volume of the RAD7 detector. From c_{air} the radon exhalation can be determined by using Eq. (2), and specific radon exhalation (M) can be calculated by Eq (3), where m is the mass of the sample.

$$E = c_{air}V \quad (2)$$

$$M = \frac{E}{m}. \quad (3)$$

However, these determined values should be considered as a minimum value due to the not negligible leakage of the passive accumulation method. Our accumulation assemblies were checked for leakage in an earlier study (Szabó, 2013) using the standard growth curve method (Girault and Perrier (2012a,b); Stoulos (2004)).

The leakage correction factors $\gamma = (\alpha + \lambda Rn)/\lambda Rn$, for the chambers were determined for our set of aluminium cans, where α stands for the radon loss rate due to leakage of the assembly. An upper estimate for the correction factor $\gamma_{max} = 2.5$ is used in this study for each accumulation chambers. Therefore we can determine the maximum specific radon exhalation values $M_{max} = \gamma_{max}M_{min}$.

The specific radon exhalation of a soil sample into water was measured by TRI-CARB 1000 TR liquid scintillation machine in two different ways. For these measurements we placed about 2 g of the original soil into a 20 ml glass vial, and then 8 ml distilled water and 10 ml OPTIFLUOR-O liquid scintillation cocktail were placed on the top. Then the vial was closed and sealed using parafilm. For the first case we monitored the actual growth of the radon concentration of the water at each 15 min for 2 days, starting at the time of preparation. This measurement allowed us to determine the very beginning of the growing curve, and the slope of the rise was determined. In the second case we measured the water radon concentration after more than 3 weeks delay when the saturation has been reached.

2.3.4. Radium activity concentration measurements by HPGe detector

The concentrations of ^{226}Ra isotopes in soil and rock samples were determined by a GC1520-7500SL coaxial type HPGe detector (energy resolution 1.8 keV at 1 MeV, detection limit (DL) 0.5 Bq kg^{-1}). The soil samples (mass between 30 g and 150 g) were placed into open cylindrical aluminium cans for measurements. The cylindrical rock samples were placed on the top of detector. The rock samples were measured two times placing on one and the other plain side to determine the reliability of the measurement. In case of soil samples for the radon exhalation and the gamma-spectroscopy measurements we used exactly the same samples in the same radon chamber.

The radium concentration was determined using the standard method of evaluating the 186 keV (^{226}Ra) peaks of the spectra (Knoll, 1989). In case of this energy gamma-photons there are no coincident photons, which would cause summing effect. The duration of each measurement was 24 h. The radioactive equilibrium between ^{238}U and ^{226}Ra was assumed and was checked using low statistics 1001 keV peak intensity. In the total count rate of the 186 keV peak was split to two parts, 58.3% of ^{226}Ra and 41.7% of ^{235}U at a radioactive equilibrium (Ebaid et al., 2005). The efficiency of the detection was calculated by Monte-Carlo simulation, which contains the self-absorption.

2.4. Rock and soil property measurements

CT analysis was carried out to determine the effective porosity of rocks. A Siemens Somatom Plus 4 CT was used in the Institute of Diagnostic Imaging and Radiation Oncology, University of Kaposvár, Hungary. First the samples were put into vacuum and then were saturated with water. Then the water content was determined using X-ray Computer Tomography (CT). The instrument has a high performance rotary anode pipe with two focuses. The X-ray beam weakened as it passed through the materials. The

Table 3b
Water chemistry results of the water samples.

Date of sampling	Ca^{2+} mg L^{-1}	Mg^{2+} mg L^{-1}	K^+ mg L^{-1}	Na^+ mg L^{-1}	HCO_3^- mg L^{-1}	Cl^- mg L^{-1}	SO_4^{2-} mg L^{-1}	NO_3^- mg L^{-1}	H_2SiO_3 mg L^{-1}
2013.04.11.	8.2	4.4	3.23	7.0	11.9	3.8	44.0	2.6	27.6
2013.09.15.	6.2	5.4	3.53	8.0	11.9	3.7	50.0	2.8	32.4
2013.10.19.	7.1	3.8	3.45	7.7	8.9	2.1	50.0	3.9	33.1

These data show that the main anion and cation concentrations at 3 sampling dates. Their uncertainties are about 5%. These values show very slight time dependence. The hydrochemical characterizaton of this water is hydrogencarbonate-chlorite-sulphate anion facies and calcium–sodium kation facies.

rate of the X-ray absorption was given in Hounsfield units (HU). The Hounsfield scale is a calibrated scale where the value of vacuum is −1024 and the water is 0. During the CT measurements 1 mm thick slices were examined and the porosity was determined for the bulk sample (Hidas et al., 2007).

The bulk density of the rock samples was determined measuring their weight using precision scale and their volume is determined by the displaced volume using a standard measuring cylinder.

To estimate the soil porosity, the physical category of the soil samples (type and texture) was estimated using hygroscopicity measurement and database search. First, we determined the hygroscopicity (hy%) following the method and the Eq. (4) of Bellúr and Varjú, 1986:

$$hy\% = \frac{m_3 - m_4}{m_4 - m_1} \cdot 100 \tag{4}$$

m_1 − the mass of the empty glassware after drying at 105C° (until constant weight)m_2 − the mass of the glassware with the ground soil samplem_3 − the mass of the glassware and the soil after 5 days in a H_2SO_4 vacuum desiccatorm_4 − the mass of the glassware and the soil after drying at 105 °C (until constant weight)

After the determination of hygroscopicity we classified the soil according to Bellúr and Varjú, 1986. To estimate the bulk density and soil porosity we used the soil database MARTHA that includes physical property values based on Hungarian soil surveys (Makó et al., 2010). We applied two conditions in the database: soil type was a forest type soil, and the texture was sandy loam. Then we estimated the bulk density over the effective porosity ratio using the average of this value from the selected dataset.

2.5. The model for estimation of potential radon content

Our principal question is whether the soil or rock around the spring is able to emit enough amounts of radon to the water to explain the measured concentrations. To decide the above question we use a slightly modified version of the radon generation rate (G) parameter (Eq. (13) in Nazaroff and Nero, 1988). In this study we use the quantity G/λ_{Rn} (I_∞) as is an upper limit for the radon concentration that can be formed in the pores under various conditions. If the pores are filled mainly by water this quantity is an upper estimate for the water radon concentration, therefore we call it here as “potential radon concentration”. This quantity is a parameter of the rocks or soil (solid phase environment) in which the water flows, and can be estimated from measuring the specific emanation quantity. This quantity is a theoretical parameter, which hardly occurs in nature due to several factors which may change radon concentration in water. Such factors are the time the water stays in the specified environment, the air content of the pores, salinity of the water, the time dependent discharge of spring water (water flow rate), the recharge of spring water by meteoric waters, radon degassing through the surface of the water table. All these factors and processes can only reduce the radon concentration relative to the potential one.

If the potential radon concentration (c_{pot}) is less than the measured one (c_{meas}) we can conclude that the given material cannot produce itself the actually measured radon concentration. On the other hand, when the potential radon concentration is higher than the measured we conclude that the material is a potential source itself of the radon in the water, however, the equilibrium may not have been reached or one or more of the above listed factors or processes had a considerable effect and reduced the concentration.

The potential radon concentration can be estimated from the minimum specific radon exhalation, density and the porosity (Eq. (5)) (Eq. (13). p 85 in Nazaroff and Nero, 1988; Eq. (1), p. 309 and Eq. (2). p. 310 in Snow and Spalding, 1997).

$$c_{pot} = \frac{M\rho}{p} \tag{5}$$

In this model p is the effective porosity of the soil/rock; M is the minimum specific radon exhalation from the measurement and ρ is the mass volume of the soil/rock. When these parameters are measured, we assume that the specific emanation and the minimum specific exhalation are the same during the measurements and that the measured samples are representative for the source area. It is necessary to consider the effective rather than the total porosity, since the closed pores do not contribute to the transport of water. For the grains of soil/rock constant radon exhalation and emanation are assumed.

A description of radon in water in three cases is developed in details in the Appendix A, B and C in Girault and Perrier, 2014. They describe the motion of radon in air, water and adsorbed phases of a fractioned zone where the discharge rate of the water is Q, and they use a three layers geological environment: rock zone, feeding zone and soil. In our case the water dominant model is useful (Appendix B). We simplify that model to a thin layer of soil with a single rock phase is the radon emanating zone. We use the equations of Appendix B without considering the time and spatial dependence of diffusion and advection, only the saturated values are used, interpreting them as a maximum of the radon concentration in water.

An important factor that can lower the radon concentration in the water phase is the presence of the air phase in the pore volume (e.g. closed air bubbles sticked to the grains). The radon then will partition between the two phases and the ratio of their concentration is governed by the κ_w, the ratio c_w/c_a in an equilibrium at a given temperature and salinity.

$$c_{w\max} = \frac{M\rho}{p_w + p_a\kappa_w} = c_{pot}\frac{p}{p_w + p_a\kappa_w} = c_{pot}\cdot a_1$$

where p_w, p_a are connected porosities filled by air and water. Since κ_w is less than 1, $a_1 < 1$, and $c_{w,max}$ is less than c_{pot}.

The residence time is crucial in reaching the equilibrium. When the water enters the soil or rock its initial radon content c_0 changes according to the Eq. (6) and reaches equilibrium in three weeks's time (assuming the partition equilibrium is achieved much faster than the radon half live).

$$c(t) < c_{UL}(t) = c_0 2^{-\frac{t}{T_{1/2}}} + c_{w,\max}\left(1 - 2^{-\frac{t}{T_{1/2}}}\right) = c_0\cdot b_0 + c_{pot}a_1 b_1. \tag{6}$$

This residence time is a function of the discharge rate. The time required for the water to flow through a fraction zone of volume V is V/Q. In case of negligible c_0 initial radon content the realistic estimate for the radon concentration is reduced from the c_{pot} values by a_1 (factor due to the radon escape to the air phase) and b_1 (time factor due to not enough time to reach radioactive equilibrium with the emanating source). Here we neglected the possibility of degassing through the water table and the mixing with water of meteoric origin. Those processes will further reduce the radon concentration. The UL symbol in the subscript of the radon concentration on the left side indicate upper limit of the concentration, due to the mentioned and further reducing factors.

3. Results

3.1. Spatial distribution of radon in the spring water

The radon concentration of the Csalóka Spring was determined in several sampling points and several times during the year. The temporal and spatial dependence of the radon concentration is shown on Fig. 3.

The highest average values were measured in point A ($c_{average} = 232 \pm 11$ Bq L^{-1}) and point E ($c_{average} = 266 \pm 13$ Bq L^{-1}). Point A is the point of discharge of the Csalóka Spring (Fig. 2b). There is a systematic difference in radon concentration of points A and B ($c_{average} = 163 \pm 9$ Bq L^{-1}) although the distance between them is small, only 25 cm. The water radon concentration is the lowest in point D (21 ± 3 Bq L^{-1}), which is the more distant one from point A. In case of point F ($c_{average} = 162 \pm 10$ Bq L^{-1}, G ($c_{average} = 45 \pm 4$ Bq L^{-1}), and H ($c = 34 \pm 5$ Bq L^{-1}) the samples originate from surface water, thus the radon concentration decreased with the distance of the discharging.

3.2. Temporal distribution of radon in the spring water

The radon concentration in the point A, was monitored during two periods to follow changes. For the first database (2007–2008) the measured values were between 161 ± 9 Bq L^{-1} and 291 ± 13 Bq L^{-1} during a year with a yearly average value of 232 ± 11 Bq L^{-1}. The empirical scattering of the data values is 41 Bq L^{-1} that is 18% of the yearly average. The 18% variability includes, however, a weak tendency of increase of the radon concentration during the year. The slope of the increase is 0.197 ± 0.076 Bq L^{-1}, which shows the minor nature of the tendency.

For the second period (2012–2013) the measured values were between 153 ± 8 Bq L^{-1} and 261 ± 12 Bq L^{-1}. The yearly average was 221 ± 5 Bq L^{-1}.

As it was already mentioned in the Section 2.5. The radon concentration in a spring water depends on the yield of discharging water, which in turn depends on the precipitation. To reveal whether there is a relationship between the radon concentration and the precipitation we collected precipitation data for the territory in the studied period of time and present the data together with the measured radon concentrations in point A on the plot in Fig. 4. We used precipitation data recorded at Görbehalom meteorological station (about 3–4 km from our sampling site) of the Hungarian Meteorological Service (Gribovszki et al., 2006).

For the first database we investigated the correlation between the radon concentration at the sampling dates, and the sum of the precipitation for a certain period (n days) before the sampling date. For the better understanding of the nature of possible correlation we calculated its dependence on the length of a summing period of $n = 2$–150 days. We calculated the n dependence of the correlation coefficients for 3 distinguished cases: A) all of the data pairs were considered, B) only the winter period (from Oct 15, 2007 to March 1, 2008) was considered, which contains the first five data pairs, C) the remaining part of the dataset, that is from March 1, 2008 to Oct 15, 2008, which covers a spring–summer–autumn period. Fig. 5 shows the resulted correlation coefficients depending on the

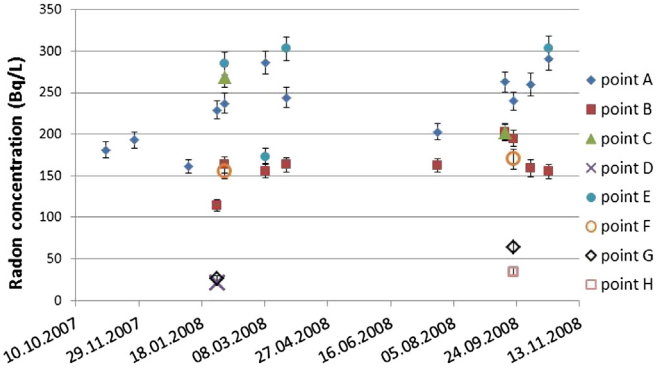

Fig. 3. Spatial and temporal distribution of the radon concentration around the Csalóka Spring. Infiltrating water directly from the soil was signed with filled symbols, and the surface water was signed with empty symbols.

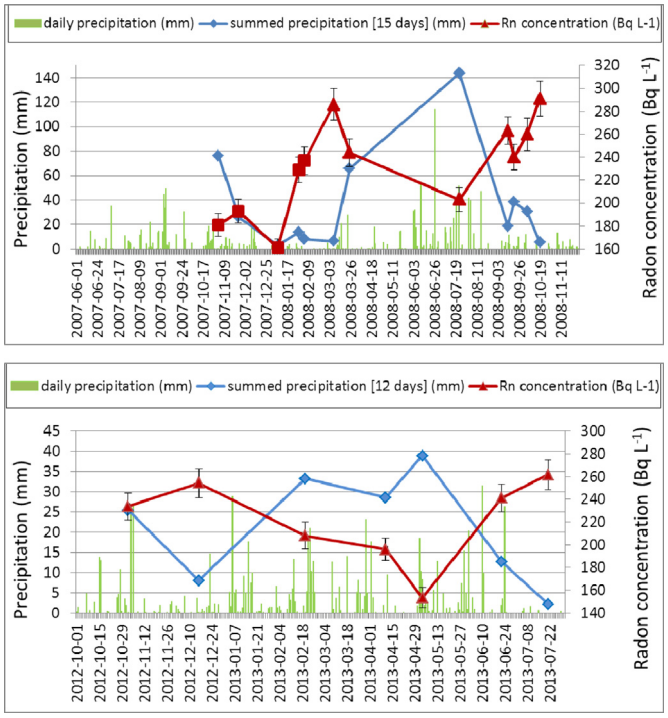

Fig. 4. Date vs. precipitation and radon concentration diagram showing temporal variation of radon concentration also as a function of precipitation. The daily precipitation values were signed with green line; the radon concentration values were indicated by red triangles. The blue line demonstrates 15 and 12-day sum of precipitation before the radon concentration measurement. (For interpretation of the references to colour in this figure legend, the reader is referred to the web version of this article.)

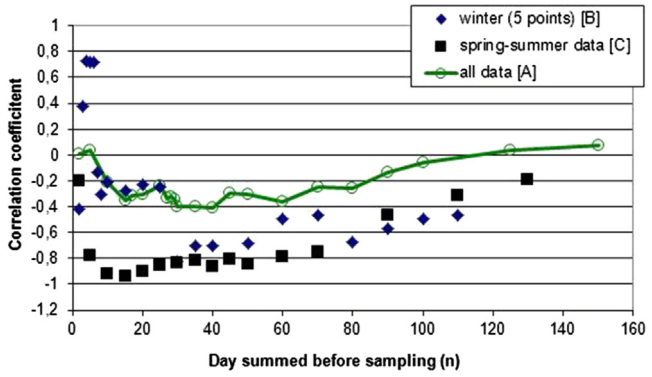

Fig. 5. The correlation coefficients vs. the summed days for 3 datasets A), B) and C) (described in the text). On the x-axis the length of the summing period for the precipitation data are shown. The solid lines are to emphasize the tendency of the correlation for the total and the summer datasets over the number of days summed.

length of the summing period for the precipitation (n). For the dataset C) every correlation coefficient is negative and for dataset A) only 10% of the values are slightly positive (within the uncertainties). The value of the negative correlation, however, depends on n. The tendency of this dependence is similar for A) and C) datasets, but for the summer period it shows significantly stronger negative correlation (solid boxes on Fig. 5). For the winter dataset the correlation does not show a standard tendency. For a short time summing (n) it is positive and for summing the precipitation for longer period it becomes negative. Furthermore it has jumps.

3.3. Radium activity concentration and radon exhalation of rocks and soils into air and radon emanation coefficients

The results of radium activity concentration, minimum radon exhalation, radon emanation coefficient of the samples and the porosity of the rocks can be seen on Table 1.

Rock samples: The radium activity concentration and radon exhalation were measured at least two times in case of all rock samples. For gamma spectroscopy each samples were placed on one side and then upside down, checking for inhomogenity. For rocks RA1, RA2 and RA3 two orientations of the plastic deformation were checked, as well (V1 and V2 samples). For radon exhalation measurements two different radon chamber were used of checking the uncertainties due to leaking.

The results of the two series of radium activity concentration measurements of 14 rock samples are shown on Fig. 6. The results of the two measurement of each sample are equal within one sigma uncertainty (except RJ1). Based on these results the method is reliable, hereinafter the value pairs were averaged (Table 1). The radium activity concentration values vary between 34 ± 3 Bq kg^{-1} and 89 ± 3 Bq kg^{-1} and their average is 65 Bq kg^{-1} for rock samples with an empirical scattering of 24%. The values of soil samples vary between 47 ± 3 Bq kg^{-1} and 145 ± 6 Bq kg^{-1} and have an average of 88 Bq kg^{-1} and empirical scattering 33 Bq kg^{-1} for the 8 soil samples.

The samples from DU are to confirm that samples, originating from debris, are representative of the surrounding rocks. The radium activity concentration values vary between 24 ± 3 Bq kg^{-1} and 99 ± 4 Bq kg^{-1} and their average is 74 ± 3 Bq kg^{-1} with an empirical scattering of 21%.

The minimum radon exhalation values averaged for two measurements of each samples placing into different chambers were determined according to 2.3.2. The highest minimum specific radon exhalation value of rock samples is between 15 ± 1 Bq kg^{-1} and 4.8 ± 0.5 Bq kg^{-1}. The average is 9 ± 1 Bq kg^{-1} and the scattering is 3.4 Bq kg^{-1}.

The average minimum specific radon exhalation of DU samples is 9.7 ± 1 Bq kg^{-1} and the scattering is 4.6 Bq kg^{-1}.

The minimum specific radon exhalation of the soil samples has higher variability than that of the rocks and ranges between 37 ± 2 Bq kg^{-1} and 5 ± 2 Bq kg^{-1}. The average is 13.3 ± 1.5 Bq kg^{-1}. The scattering is 10.7 Bq kg^{-1}. The radon emanation coefficient in case of soils and rocks is 14 ± 2% including DU results (Table 1).

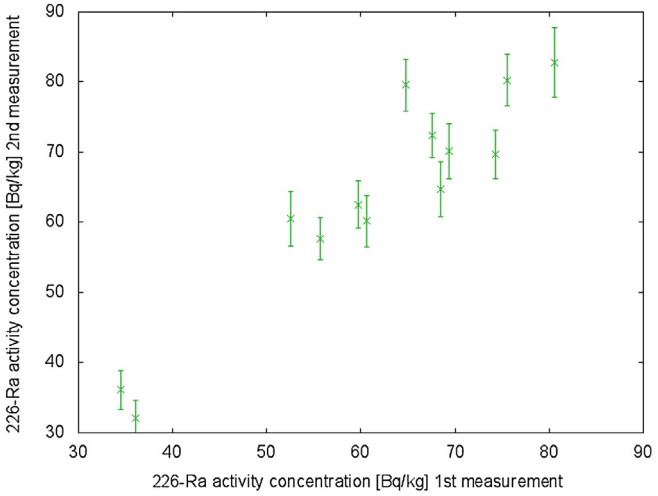

Fig. 6. The value of the first radium activity concentration measurement as a function of the value obtained with the second measurement.

3.3.1. Radon exhalation into water

As a comparison of the exhalation into air and into water the specific radon emanation was determined in two ways, as described in Section 2.3.2. For a soil sample SA1w. For the rock samples this measurement were not carried out because the exhalation vial is too small to put representative amount of rock in it. The exhalation into water determined two ways; from the slope was 7.8 ± 1.8 Bq kg^{-1} and from two radioactive equilibrium measurements were 10.3 ± 1.9 Bq kg^{-1} and 9.3 ± 1.9 Bq kg^{-1}. The average of these values was accepted as a representative for the sample: 9.1 ± 1.5 Bq kg^{-1}.

3.4. Porosity of rock samples

The porosity of the rock samples was determined with CT measurements. We found that the porosity is between 0.84% and 1.35% with an average of 1.21% and the empirical scattering is 0.31%. The measured values can be seen in the last column of Table 1.

3.5. Physical properties of soil samples

The measured values of the hygroscopicity were found to be between 1.02% and 1.25%. According to these values the classification of the soil samples is sandy loam. The soil type was determined due to in situ observations and soil map information which resulted in brown forest type. In the Hungarian soil database (Makó et al., 2010) we applied a selection for i) location is Sopron mountains, ii) soil type is brown forest soil and iii) USDA texture is sandy loam. 140 data were found at 3 sites in the database. We calculated the average of bulk density over effective porosity ratios for the three areas and found 3.81, 4.05, 3.07. The average of these is 3.6 ± 0.5 and the empirical scattering is 14%. The variance of the bulk density and porosity values used in the dataset were about 10%, which corresponds also to the 14% uncertainty of the calculated ratio.

3.6. Estimation of the potential radon concentration

For rocks the minimum specific radon exhalation is 10.1 ± 1.0 Bq kg^{-1}, the average porosity is 1.21% and the bulk density is 2.42 g cm^{-3}. From these data we obtained 2020 Bq L^{-1} averaged potential radon concentration for the rock samples from point A (empirical scattering 680 Bq L^{-1}, which is 34%).

For soil samples we determined the average minimum specific exhalation values for points A, B and D and the results are 7.9 ± 2.3 Bq kg^{-1}, 25 ± 17 Bq kg^{-1} and 4.6 ± 0.6 Bq kg^{-1} respectively (the empirical scatterings are shown as uncertainties, here). The porosity of the soils is 43% and the bulk density is 1.45 g cm^{-3}.

The maximum specific radon exhalation values are estimated using an upper limit for leakage parameter $\gamma_{max} = 2.5$. Therefore the potential radon concentration can be calculated in two ways. An upper and a lower estimate can be given $c_{pot,min}$ and $c_{pot,max}$. We estimate an about 20% cumulative uncertainty for these values.

The yearly average of the water radon concentrations were

determined for 3 sampling points: A, B, D. The point A is the discharge point, B and D are locations where water seepage was observed and sampling was possible. We calculated the potential radon concentrations for these three points according to the results of minimum and maximum specific radon exhalation, the porosity and bulk density of soils and rocks using Eq. (5).

The potential radon concentrations are in all cases lower than the measured radon concentration (26.8 Bq L^{-1}, 85.0 Bq L^{-1} and 15.6 Bq L^{-1} respectively (Table 2).

3.7. Physical–chemical properties of the water samples

The flow rate of this spring is rather low. Its measurement includes a high uncertainty of collecting the total volume of the discharging water. At one sampling day we measured the flow rate 3 times. The average and the empirical scattering were found 9 ± 3 mL/s.

The physical–chemical parameters for A point of Csalóka-Spring obtained during the second period are shown in Table 3.

4. Discussion

Csalóka Spring has the highest water radon concentration locally around the Sopron Mountains (average of 227 ± 10 Bq L^{-1} according to two measuring period). The radon concentration of other springs varies between 10 and 160 Bq L^{-1} (Aros, 2003). However the radon concentration level in Csalóka Spring is an ordinary value for springs and wells on gneiss or granite bedrock, which is typically between 23 and 1400 Bq L^{-1} (Banks et al., 1998; Horváth et al., 2010; Przylibski, 2000; Cosma et al., 2008; Vinson et al., 2009).

The rocks in a 10 m radius around the Csalóka Spring are deformed gneisses. They showed an average radium concentration of 65 ± 4 Bq kg^{-1}. This is higher than the ones measured in metagranites (33 ± 3 Bq kg^{-1}) and deformed gneisses (53 ± 4 Bq kg^{-1}) in the Sopron Mountains (Freiler et al., 2015). This value seems to be close to an average compared to the gneissic and granitic rocks in the Sudety Mountains (34–132 Bq kg^{-1}; Przylibski, 2000).

The average radium content in the soil samples around the Csalóka Spring was higher, than that of the rock samples (88 ± 4 Bq kg^{-1}). This value is more than two times higher than the average radium activity concentration in soils in Hungary (33 Bq kg^{-1}) (UNSCEAR, 2000).

The radon emanation coefficients were in the range of 5–32% with an average of 14.1%, and 14% for soil and rock samples respectively. These data show, that the rock samples have about the same emanation coefficient as the soils have. It is not a usual behaviour, since generally the soils have higher emanation coefficients than the rock samples (Sakoda et al., 2011). This larger emanation coefficient of these deformed gneiss rock samples can be due to the shearing and deformation, which opened cracs and communicating pores. These serve as pathways for migration of radon, as also pointed out by Wanty et al. (1992).

We made model calculations from the measured minimum exhalation properties of rock samples found on the surface around the spring to show the possible source of radon in water. These calculations revealed that the minimum and maximum estimate for the potential water radon concentration, which may be provided by the country rock at the main discharge location (point A), is 2020 and 5050 Bq L^{-1}.

Even the conservative (lower) estimate is about 9 times higher than the measured average value of 227 ± 10 Bq L^{-1}. This potential radon concentration is 7 times higher than even the maximum of the measured water radon concentration at point A (291 Bq L^{-1}). Considering the uncertainties of the model and the calculated and measured values, this means that the rocks can be the source of the radon in water. However, the large difference is attributed to the several factors that reduce the radon concentration in the water in the real situation. The discharge for example, determines whether the water stays enough time in the emanating environment. If the discharge is large enough the radioactive equilibrium between the emanation and the radon activity will not be reached. Another reducing factor is the recharge by the meteoric water. We emphasize the effect of this process is reducing the radon concentration in the spring water. After the rainy periods in summer about 160 Bq L^{-1} radon concentrations were measured (see later), which is about the half of the maximum value, appeared after dry periods (about 290 Bq L^{-1}). The open nature of the subsurface water reservoir may also lead to radon loss in water, which may be a further cause of the measured lower radon concentration of the spring water. These processes all reduce the radon concentration in water. That is the reason why we found lower concentration then the calculated potential radon concentration from the emanation properties.

On the other hand the crude maximum estimate for the calculated potential radon concentration of the soil samples (65 ± 15 Bq L^{-1}) around point A are 3.5 times less than the measured average value, and 2.5 times less than the minimum of measured values (161 Bq L^{-1}). This means that the soil is capable of providing just a small part of the radon concentration in the spring water. The soil cannot be the origin of the water here.

At points B and D the maximum estimate for the potential radon concentration is higher than the average values, therefore we cannot discard the soil as an origin at these points. But these points are 1–3 m far from the main discharge location, their flow rate is considerable lower. Their radon content can be far less than the water radon concentration deep in the flow due to e.g. degassing to the open air while staying on the surface.

The emanation properties of the rock here produced so much higher potential radon concentration then the soil, thus the simplified model was enough to distinguish which is the source of radon in this case.

The measured radon concentration values between 2007 and 2008 of the Csalóka Spring in point A, ranges from 161 Bq L^{-1} to 291 Bq L^{-1}, during a year showing an empirical scattering of 41 Bq L^{-1}, that is 18% of the yearly average. Between 2012 and 2013 the measured values ranges from 153 Bq L^{-1} to 261 Bq L^{-1}. The yearly average was 221 ± 5 Bq L^{-1}. The empirical scattering is 38 Bq L^{-1}, that is 17% of the yearly average. This low variability demonstrates that the hydrogeological environment has dominating role in the level of radon concentration. Other factors like e.g. distribution of the yearly precipitation and the corresponding yield of the spring may account for the changes. A clear dependence of radon concentration on the summed precipitation in the spring–summer–autumn (referred to as "summer") period is demonstrated on Figs. 4 and 5.

For the first period the "summer" dataset "C)" shows a negative correlation, independently from the length of the summing period. The strongest negative correlation (−0.94) was found if we used $n = 15$ days. For the second period the strong negative correlation was found, too, it is −0.91, when $n = 12$ days. The time delay is due to the time needed for the meteoric water to infiltrate and reach the radon rich subsurface flow.

One explanation for the negative correlation is that the precipitation dilutes the subsurface waters due to infiltration. The infiltrated water may have several pathways, with the consequence of different contact time with the radon emanating country rock. If we take into account that 21 day necessary for saturation of the water in respect of radon at the level of 2020 Bq L^{-1}, and the shape of the saturation curve, we assume that most of the infiltrating

water does not spend more than 3 days in this subsurface environment. As this residence time is much smaller than the one calculated from the best correlation (15 days) we assume that a big part of the subsurface rock and soil surrounding the water pathways have much less radon emanation potential than the deformed gneiss at the discharge point of the Csalóka Spring.

There are another possible factors that can have an effect on the correlation between the radon concentration and the precipitation. This is the effect of the velocity of the groundwater flow at certain geological circumstances, where the size of the radon emitter rocks is smaller than the length of the groundwater route in 21 days. In the low precipitation period the water discharge is lower, and the τ parameter can reach higher values, filling the groundwater with more radon in the slow flow, since the water is in contact with the radon emitter wall rock for a longer time, and more radon atoms could diffuse to the water.

Our data give no possibility to distinguish between these possibilities, but the yearly tendency can be explained overall by the fact that we started our measurements in a wet period (more dilution) of the year, and the following dry periods made the radon concentration higher as a tendency, even though there was another short wet time during the summer.

On the contrary in the winter period the precipitation is not a decisive factor, there is no correlation with the water radon concentration. A possible reason is that the infiltration of the solid precipitation cannot be predicted. As an overall result we state that the consecutive dry and wet periods make a yearly average radon concentration of the spring, and there is a variability of only 20% around this average. A long term meteorological changes however can change the yearly average.

The measured water radon concentrations in the points around the Csalóka Spring show significant spatial differences (Figs. 2 and 3). We measured the highest values at the discharge points of A and E. On the contrary at point D, which is topographically the highest point where the water was sampled the measured radon concentration is only 21 ± 3 Bq L^{-1}. Low radon concentrations were also measured in points G and H. The low concentrations in points G and H may be explained by degassing, although water in points G and H represent the spring water.

There is a significant difference between points A and B in spite of the relative proximity of the two points. The explanation is that in point B the spring water is mixing with the stored water in the soil, which has much lower radon concentration compared to point A. The measured and the calculated radon concentrations from soil exhalation show inequilibrium in points A, B and D. E.g. in point B, if the water was stored in the soil for three weeks (to reach equilibrium), the radon concentration would be 83 Bq L^{-1}, but the measured radon concentration is 163 Bq L^{-1}. This means that mixing of water with higher radon concentrations from the spring water causes higher concentrations than the equilibrium one. This applies for points A and D as well (see Table 2).

5. Conclusions

We determined the yearly dataset of radon concentration in the water of the Csalóka Spring. We also investigated the radon emanation parameters, porosity and bulk density of the deformed gneissic rocks and soils around Csalóka Spring to be able to explain the origin of the radon concentration level in the spring (2 years average 227 ± 10 Bq L^{-1}). The emanation properties of the rock found here produced so much higher potential radon concentration then the soil, thus the simplified model was enough to distinguish that the rock is the source of radon in this case.

We obtained that the radon concentration in the water depends on several factors, first of all on the radon emanation properties of the country rock. But the demonstrated time dependence shows other factors are also important. For example the varying travel time of the water in the pores of the rock and the seasonal changes in the quality and the amount of precipitation caused 18% changes in the radon concentration in the studied year.

The average radium concentration of 65 ± 4 Bq kg^{-1} measured from the deformed gneiss around the Csalóka Spring and calculated the emanation coefficient of 14% and porosity of 1% made it possible to estimate the potential radon concentration of at least 2020 ± 400 Bq L^{-1} in the country rock. The relatively high emanation coefficient is due to the increased effective porosity by the plastic deformation of the gneiss. As the water contains less than 1/9ths of that value, we assume that dilution by the infiltrating meteoric waters can be important and/or the travel time of the water was much less than 21 days which is necessary to reach the radioactive equilibrium between the water and the country rock. One possible reason of the short transit time can be that the measured high radon emission parameters refer to only a small volume of the country rock close to the surface.

Acknowledgements

The authors thank Mihály Kucsara – University of West Hungary – to enable and provide precipitation data, and András Makó – Institute for Soil Sciences and Agricultural Chemistry, Centre for Agricultural Research, Hungarian Academy of Sciences – to make it possible to use the MARTHA database for our work. Thank for Csaba Szabó and the crew of Lithosphere Fluid Research Laboratory (LRG) at Eötvös University and Judit Mádl-Szőnyi, Anita Erőss to the help with the water chemistry measurements and fruitful discussions on hydrogeologycal questions.

Special thanks to Tibor Horváth, who helped to carry out all of the sampling.

References

Akerblom, G., Lindgren, J., 1996. Mapping of ground water radon potential. In: IAEA Technical Committee Meeting, Vienna, Austria.
Al-Masri, M.S., Blackburn, R., 1999. Radon-222 and related activities in surface waters of the English Lake District. Appl. Radiat. Isot. 50, 1137–1143.
Andrews, J.N., Wood, D.F., 1972. Mechanism of radon release in rock and matrices and entry into groundwater. Inst. Min. Metall. Trans. 81, B198–B209.
Aros, G., 2003. A természetes radioaktivitás vizsgálata a Soproni-hegységben. Eötvös University, Department of Atomic Physics. Thesis.
Banks, D., Frengstad, B., Midtgard, A.K., Krog, J.R., Strand, T., 1998. The chemistry of Norwegian groundwaters: I. The distribution of radon, major and minor elements in 1604 crystalline bedrock groundwaters. Sci. Tot. Environ. 222, 71–91.
Bellúr, P., Varjú, P., 1986. Talajvizsgálati módszerek (Manuscript).
Breitner, D., Arvela, K.H., Hellmuth, T., Renvall, T., 2010. Effect of moisture content on emanation at different grain size fractions – a pilot study on granitic esker sand sample. J. Environ. Radioact. 101, 1002–1006.
Cosma, C., Moldovan, M., Dicu, T., Kovacs, T., 2008. Radon in water from Transylvania (Romania). Radiat. Meas. 43, 1423–1428.
Csige, I., 2003. Radon a környezetben. In: Kiss, A.Z. (Ed.), Fejezetek a környezet fizikából. Debrecen, pp. 123–145.
Draganits, E., 1998. Two crystalline series of the Sopron Hills (Burgenland) and their correlation to the lower Austroalpine in Eastern Australia. Jb. Geol. B. A 141, 113–146 (in German with English abstract).
Durridge Company Inc, 2000. RAD7 Electronic Radon Detector. User Manual.
Eaton, A.D., Clesceri, L.S., Rice, E.W., Greenberg, A.E., Franson, M.A.H. (Eds.), 2005. Standard Methods for the Examination of Water and Wastewater, 21st edition. American Public Health Association, Washington DC.
Ebaid, Y.Y., El-Mongy, S.A., Allam, K.A., 2005. ^{235}U–γ emission contribution to the 186 keV energy transition of ^{226}Ra in environmental samples activity calculations. Int. Congr. Ser. 1276, 409–411.
European Commission, 2001. Commission Recommendation of 20th December 2001 on the Protection of the Public against Exposure to Radon in Drinking Water Euratom2001/982/, L344/85.
Freiler, Á., Horváth, Á., Török, K., 2015. ^{226}Ra activity distribution of rock in the Sopron Mts. (West-Hungary). J. Radioanal. Nucl. Chem. 303, Nr 2. http://dx.doi.org/10.1007/s10967-014-3914-3.
Girault, F., Perrier, F., 2012a. Measuring effective radium concentration with large numbers of samples. Part I – experimental method and uncertainties. J. Environ. Radioact. 113, 177–188.

Girault, F., Perrier, F., 2012b. Measuring effective radium concentration with large numbers of samples. Part II – general properties and representativity. J. Environ. Radioact. 113, 189–202.
Girault, F., Perrier, F., 2014. The Syabru-Bensi hydrothermal system in central Nepal: 2. Modeling and significance of the radon signature. J. Geophys. Res. Solid Earth 119, 4056–4089. http://dx.doi.org/10.1002/2013JB010302.
Gribovszki, Z., Kalicz, P., Kucsara, M., 2006. Streamflow characteristics of two forested catchments in sopron Hills. Acta Silv. Lig. Hung. 2, 81–92.
Gundersen, L.C.S., Wanti, R.B., 1991. Field studies of radon in rocks, soils and waters. U.S. Geol. Surv. Bull. 39–50. http://energy.cr.usgs.gov/radon/shear1.html.
Hidas, K., Falus, Gy., Szabó, Cs., Szabó, P.J., Kovács, I., Földes, T., 2007. Geodynamic implications of flattened tabular equigranular textured peridotites from the Bakony-Balaton Highland volcanic field (Western Hungary). J. Geodyn. 43, 4–5.
Horváth, Á., Sajo-Bohus, L., Urbani, F., Marx, G., Piróth, A., Greaves, E.D., 2010. Radon concentrations in hot spring waters in northern Venezuela. J. Environ. Radioact. 47, 127–133.
Kisházi, P., Ivancsics, J., 1987. A Soproni Csillámpala Formáció genetikai kőzettana. Földtani közlöny 117, 203–221.
Kisházi, P., Ivancsics, J., 1989. A Soproni Gneisz Formáció genetikai kőzettana. Földtani közlöny 119, 153–166.
Knoll, G.F., 1989. Radiat. Detect. Meas. John Wiley & Sons Inc.
Lelkes-Felvári, Gy, Sassi, F.P., Visoná, D., 1984. Pre-Alpine and Alpine developments of the Austridic basement int he Sopron area (Eastern Alps, Hungary). Rend. Soc. It. Miner. Pet. 39, 593–612.
Makó, A., Tóth, B., Hernádi, H., Farkas, Cs., Marth, P., 2010. Introduction of the Hungarian detailed soil hydrophysical database (MARTHA) and its use to test external pedotransfer functions. Agrokém. Talajt. 59 (1), 29–38.
Nazaroff, W.W., Nero Jr., A.V., 1988. Radon and Its Decay Products in Indoor Air. John Wiley & Sons, United States of America.
Onishchenko, A., Zhukovsky, M., Veselinovic, N., Zunic, Z.S., 2010. Radium-226 concentration in spring water sampled in high radon regions. Appl. Radiat. Isot. 68, 825–827.
Przylibski, T.A., 2000. Estimating the radon emanation coefficient from crystalline rocks into groundwater. Appl. Radiat. Isot. 53, 473–479.
Przylibski, T.A., Mamont-Ciesla, K., Kusyk, M., Dorda, J., Kozlowska, B., 2004. Radon concentrations in groundwaters of the Polish part of the Sudety Mountains (SW Poland). J. Environ. Radioact. 75, 193–209.
Sakoda, A., Ishimori, Y., Yamaoka, K., 2011. A comprehensive review of radon emanation measurements for mineral, rock, soil, mill tailing and fly ash. Appl. Radiat. Isot. 69, 1422–1435.
Samuelsson, C., 1990. The closed-can exhalation method for measuring radon. J. Res. Natl. Inst. Stand. Technol. 95 (2), 167–169.
Samuelsson, C., Erlandsson, K., 1988. The Implication of the Time-dependent Diffusion Theory on Radon-222 Exhalation Measurements. Radiation Protection Practice, II. Sydney. Pergamon Press, p. 898.
Samuelsson, C., Petterson, H., 1984. Exhalation of ^{222}Rn from porous materials. Radiat. Prot. Dosim. 7 (1–4), 95–100.
Snow, D.D., Spalding, R.F., 1997. Short-term aquifer residence times estimated from ^{222}Rn disequilibrium in artificially-recharged ground water. J. Environ. Radioact. 37/3, 307–325.
Somlai, K., Tokonami, S., Ishikawa, T., Vancsura, P., Gáspár, M., Jobbágy, V., Somlai, J., Szabó, Zs, Szabó, Cs., Horváth, Á., 2011. Comparison of two ^{222}Rn mass exhalation rate measurement methods by study of Hungarian adobe building materials. In: Nordic Society for Radiation Protection Conference: Current Challenges in Radiation Protection, August 22–25, 2011, Reykjavik, Iceland.
Soonawala, N.M., Telford, W.M., 1980. Movement of radon in overburden. Geophysics 45, 1297–1315.
Stoulos, S., Manolopoulou, M., Papastefanou, C., 2004. Measurement of radon emanation factor from granular samples: effects of additives in cement. Appl. Radiat. Isot. 60, 49–54.
Szabó, Zs, 2013. Terrestrial Radioactivity in Hungarian Adobe Building Material and Dwellings with a Focus on Thoron. PhD Thesis. http://teo.elte.hu/minosites/ertekezes2013/szabo_zsuzsanna.pdf.
Tanner, A.B., 1980. Radon migration in the ground: a supplementary review. In: Gesell, T.F., Lowder, W.M. (Eds.), The Natural Radiation Environment III. Symposium Proceedings Houston, April 1978, pp. 5–56.
Török, K., 1998. Magmatic and high pressure metamorphic development of orthogneisses in the Sopron area, Eastern Alps (W-Hungary). N. Jb. Miner. Abh. 173, 63–91.
Török, K., 1999. Pre-Alpine development of the andalusite-sillimanite-biotite-schist from the Sopron-Mountains (Eastern Alps, W-Hungary). Acta Geol. Hung. 42 (2), 127–160.
Török, K., 2001. Multiple fluid migration events in Sopron Gneisses during the Alpine high-pressure metamorphism, as recorded by bulk-rock and mineral chemistry and fluid inclusions. N. Jb. Miner. Abh. 177 (1), 1–36.
UNSCEAR Report, 2000. Sources and Effects of Ionising Radiation, UN, New York.
Vinson, D.S., Vengosh, A., Hirschfeld, D., Dwyer, G.S., 2009. Relationships between radium and radon occurrence and hydrochemistry in fresh groundwater from fractured crystalline rocks, North Carolina (USA). Chem. Geol. 260, 159–171.
Wanty, R.B., Lawrence, E.P., Gundersen, L.C.S., 1992. Theoretical model for the flux of radon from rock to ground water. In: Gates, A.E., Gundersen, L.C.S. (Eds.), Geologic Controls of Radon, Special Paper 271. The Geological Society of America, pp. 73–78.
Weise, S.M., Bräuer, K., Kämpf, H., Strauch, G., Koch, U., 2001. Transport of mantle volatiles trough the crust traced by seismically released fluids: a natural experiment in the earthquake swarm area Vogtland/NW Bohemia, Central Europe. Techtonophysics 336, 137–150.